*Int. J. Heat Mass Transfer.* Vol. 14, pp. 133–140. Pergamon Press 1971. Printed in Great Britain

# THE SLUG EXPULSION OF FREON-113 BY RAPID DEPRESSURIZATION OF A VERTICAL TUBE

**W. D. FORD* and HANS K. FAUSKE**

Reactor Engineering Division, Argonne National Laboratory, Argonne, Illinois, U.S.A.

**and S. G. BANKOFF**

Chemical Engineering Department, Northwestern University, Evanston, Illinois, U.S.A.

(*Received* 11 *February* 1970 *and in revised form* 24 *April* 1970)

**Abstract**—Experimental data, ranging in initial superheat from 59 to 128°F, has been obtained for the slug expulsion of Freon-113 from a constant-diameter channel. In addition, an analysis is given in which the energy and momentum equations are coupled numerically. The energy equation accounts for not only the energy transported across the upper and lower liquid–vapor interfaces, but also that transported across the wall film–vapor interface. In computing the energy contribution of the wall film, a thin surface thermal boundary layer was assumed to exist, whose thickness as a function of exposure time and position along the vapor space was taken into account. The agreement between the experimental data and coupled solution was found to be good.

## NOMENCLATURE

$\alpha$, thermal diffusivity of liquid [ft$^2$/s];
$\lambda$, latent heat of vaporization [Btu/lb];
$\rho_v$, vapor density [lb/ft$^3$];
$\rho_L$, liquid density [lb/ft$^3$];
$\xi_1, \xi_2, \sigma$, distance within liquid slugs and film normal to vapor–liquid surface [ft];
$\phi(\tau)$, interface temperature [°F];
$A$, cross sectional area of coolant channel [ft$^2$];
$A'$, surface area of wall film [ft$^2$];
$f$, single phase coefficient of friction;
$F$, frictional force [lb$_f$];
$g$, acceleration due to gravity [ft s$^2$];
$\hat{H}_v$, enthalpy of vapor [Btu/lb];
$\hat{H}_L$, enthalpy of liquid [Btu/lb];
$L$, constant diameter channel length [ft];
$L'$, length of liquid in channel and plenum [ft];
$P_{L'}(t)$, pressure above plenum [lb$_f$/ft$^2$];
$P_g(t)$, pressure within vapor space [lb$_f$/ft$^2$];
$Q$, volumetric heat generation rate in liquid slugs [Btu/ft$^3$s];
$T(\xi, t)$, temperature within liquid slug [°F];
$T_w$, wall temperature [°F];
$\Delta x(t)$, length of vapor space [ft];
$v(t)$, velocity [ft/s];
$x_1(t)$, position of upper liquid–vapor interface [ft].

## INTRODUCTION

THE EXPULSION of liquid metals from a blocked channel has received considerable attention in the safety analysis of fast reactors. The experimental problems involved in working with liquid metals are such that the use of non-metallic fluids in obtaining data from which models may be deduced appears attractive. In addition, non-metallic fluids enable visual observation of the flow regime during the expulsion.

* Also at Chemical Engineering Department, Northwestern University, Evanston, Illinois.

Spiller *et al.* [1] have performed several experiments with liquid potassium in which they verified not only a slug-type expulsion, but also the existence of a thin liquid film adhering to the wall of the channel during the expulsion. Several computer codes have been developed describing this form of expulsion [2, 3].

Kosky [4] used a rapid depressurization technique in achieving slug expulsions in water. The expulsion was observed through the use of high-speed photography. In his analysis Kosky estimated the rate of void growth from a modification of the Plesset and Zwick [5] single-bubble analysis. It was assumed that the pressure in the upper plenum was constant during the growth of the void, so that the fluid superheat could be precisely defined. Board [6] similarly examined expulsion rates in both single-channel and multi-pin geometries. The test fluid was again water. Before initiating the expulsion, the system was slowly depressurized until the desired superheat was achieved. The bubble formation was then triggered by either a laser beam or wire electrode. Hence, the liquid superheat was well-defined when the bubble growth was initiated.

In his analysis, which closely follows that of Kosky, Board did not account for the variation in the thickness of the thermal boundary layer as a function of exposure time along the length of the vapor space. Figure 1 illustrates the difference between Board's solution and a modification of that solution which accounts for the axial variation in the thermal boundary-layer thickness. More details are given below. It was not possible to couple the energy and inertia equations in this case, owing to a lack of information on the height of liquid above the bubble at the time of nucleation.

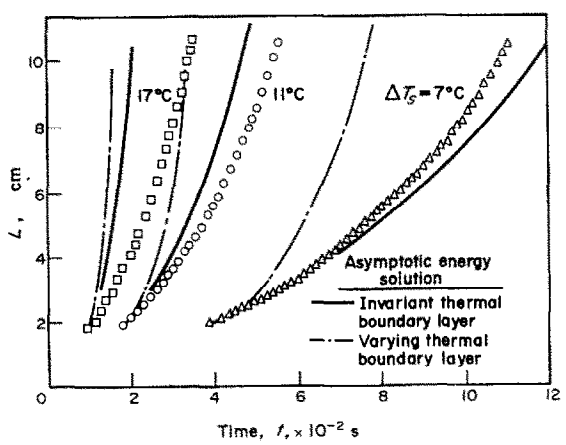


FIG. 1. Comparison of asymptotic energy solutions with experimental data from [6].

The present work employs Freon-113, rather than water, for depressurization studies. It has been found from experience that Freon-113 wets glass very well, and can sustain a high superheat with only nominal cleansing of the glass. With water, extensive degassing and cleansing of the glass is necessary. Thus, Freon-113 facilitates the investigation of a wide range of superheat.

Additionally, in this study the energy solution of Kosky and Board is modified to include the effect of the variation in the thermal boundary-layer thickness as a function of exposure time, and is coupled with the inertia controlled solution. This provides a general model for slug expulsion in which it is no longer necessary to select an initial vapor length.

## EXPERIMENT

The technique employed in this work to initiate bubble growth was that of rapid depressurization. Figure 2 illustrates the depressurization facility.

The apparatus consisted of a large vacuum vessel ($\sim 50$ ft$^3$) to which a test section could be attached, separated by an aluminium diaphragm. Figure 3 illustrates the test section with all appropriate dimensions.

The test section consisted of a constant-diameter tube and a variable diameter plenum. The plenum and upper portion of the test section were provided with a cooling jacket; the bottom was enclosed within a heating jacket. Piezoelectric pressure transducers were mounted at the top and bottom of the test section, which monitored the pressure throughout the event.

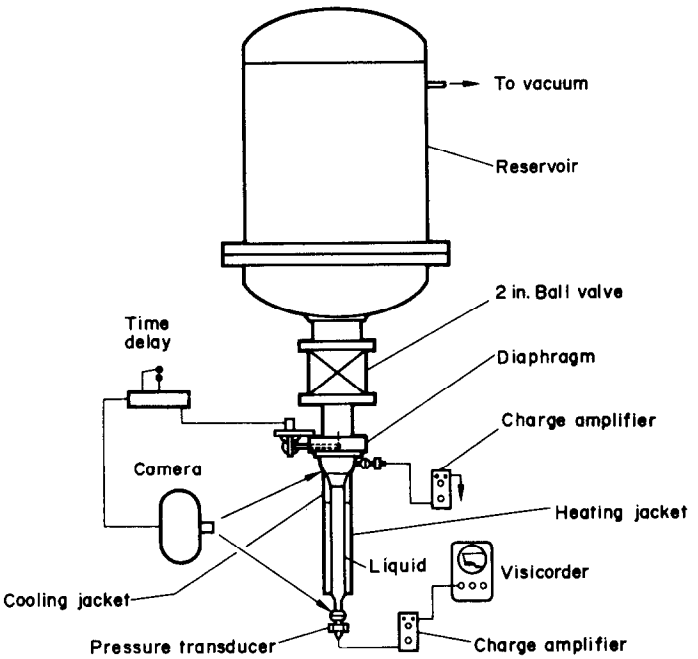


FIG. 2. Experimental test facility.

By comparing the high-speed film and pressure trace, the pressure at the time of nucleation could be determined.

The test began by filling the channel and plenum with Freon-113 while both the cooling and heating jackets were at ambient temperature. The receiver vessel was then evacuated, and the cooling and heating water flows turned on. When the temperature within the test section had reached that of the jacket, the expulsion was initiated through a time-delay system, which first started the high-speed camera and allowed it to come up to speed (2000 frames per s). The oscillograph monitoring pressure traces was then started and allowed to reach a constant speed (80 in. per s), after which the aluminium diaphragm was ruptured by a solenoid-actuated knife edge. The cooling and heating times were kept as low as possible in order to minimize convective effects.

## EXPERIMENTAL DATA

Figure 4 illustrates various stages in the growth of the vapor space during an expulsion. The high-speed camera used in filming the event was wired to a timing device which provided marks along the edge of the film every millisecond. The films were analyzed frame by frame on a motion analyzer.

The pressure trace mounted at the top of the test section was used in conjunction with the high-speed film to determine the plenum pressure history during the growth of the vapor space.

In none of the events recorded was vaporization from the plenum interface noticeable.

## ANALYSIS

The mathematical analysis for a slug-type expulsion will now be considered. Figure 5 shows the channel configuration.

The one-dimensional incompressible equation of motion may be written between planes (1) and (2) in Fig. 5 as

$$\rho_L \frac{\partial v}{\partial t} = -\frac{\partial P}{\partial x} - \frac{F}{A} - \rho_L g. \qquad (1)$$

The assumption is made that the slug begins as an infinitesimally small strip occupying the entire channel with the exception of any film

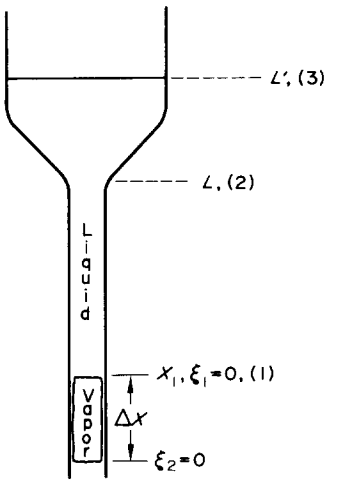


FIG. 5. Model for slug type expulsion.

remaining on the wall. Equation (1) may now be integrated from plane (1) to plane (2) to yield after simplification

$$\frac{\partial v}{\partial t} = \frac{(P_g - P_L)g_c}{\rho_L(L - x_1)} - \frac{2v^2 f}{D} - g. \tag{2}$$

To estimate the pressure at $x = L$, the frictionless Bernoulli equation is applied between planes (2) and (3)

$$P_L = P_{L'} - \frac{\rho_L v^2}{2g_c} + \frac{\rho_L g}{g_c}(L' - L). \tag{3}$$

Equations (2) and (3) may be solved for $v(t)$ providing the pressure in the vapor space, $P_g$, is known as a function of time. This is obtained from an energy balance for the vapor space in Fig. 5. Assuming a uniform, thin, stationary liquid film exists at the channel walls, a macroscopic energy balance yields,

$$\rho_v \lambda A \frac{\partial \Delta x}{\partial t} + A\Delta x \frac{\partial(\rho_v \hat{H}_v)}{\partial t} = kA \left.\frac{dT(\xi_1,t)}{d\xi_1}\right|_{\xi_1=0} + kA \left.\frac{dT(\xi_2,t)}{d\xi_2}\right|_{\xi_2=0} + k\int_{A'} \left.\frac{dT(\sigma,t)}{d\sigma}\right|_{\sigma=0} dA' + A\Delta x \frac{\partial P}{\partial t} \tag{4}$$

where the temperature gradient at the liquid film surface depends upon the time at which the fluid elements were exposed to the vapor.

The temperature gradients at the upper and lower liquid–vapor interfaces are found by assuming plug flow in the upper and lower slugs of liquid. The heat equation for the upper slug may be written, neglecting radial gradients, in the form

$$\alpha \frac{\partial^2 T(\xi_1,t)}{} + \frac{Q(\xi_1,t)}{\rho_L C_p} = \frac{\partial T(\xi_1,t)}{\partial t} \tag{5}$$

subject to

$$T(\xi_1, 0) = F(\xi) \tag{6a}$$

$$T(0,t) = \phi(t) \tag{6b}$$

$$T(\infty,t) < \infty. \tag{6c}$$

The temperature gradient at the liquid–vapor interface is found to be

$$\left.\frac{dT(\xi_1,t)}{d\xi_1}\right|_{\xi_1=0} = -\int_0^t \frac{1}{\sqrt{[\pi\alpha(t-\tau)]}} \frac{d\phi(\tau)}{d\tau} d\tau + \int_0^\infty\int_0^t \frac{\xi_1}{2k\sqrt{[\pi\alpha(t-\tau)^3]}} \exp\left[\frac{-\xi_1^2}{4\alpha(t-\tau)}\right] + Q(\xi_1,t)\, dt\, d\xi_1 \int_0^\infty \frac{T(\xi_1,0)}{2\alpha} \frac{\xi_1}{\sqrt{[\pi\alpha t^3]}} \exp\left[\frac{-\xi_1^2}{4\alpha t}\right] d\xi_1 - \frac{\phi(0)}{\sqrt{[\pi\alpha t]}}. \tag{7}$$

The first term expresses the influence of the temperature history of the liquid–vapor interface; the second of the distributed heat source, (which, in fact, represents the heat input to the liquid slug from the walls); and the final terms express the dependence upon the initial conditions. Note that $\phi(\tau)$ is determined by the pres-

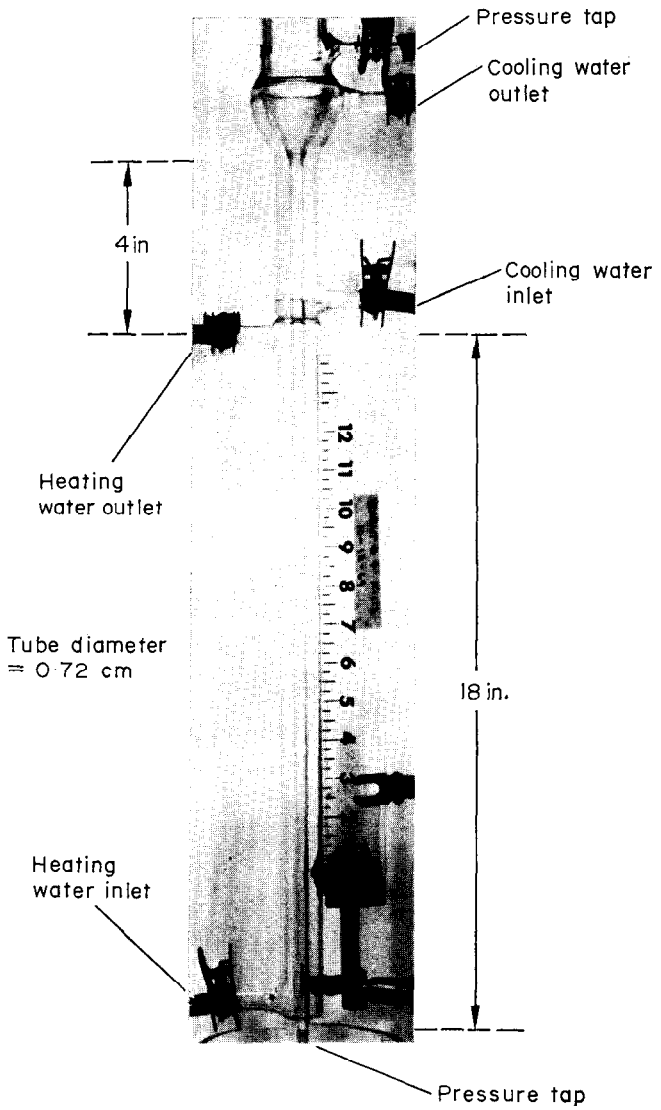


FIG. 3. Experimental test section.



[facing page 136]

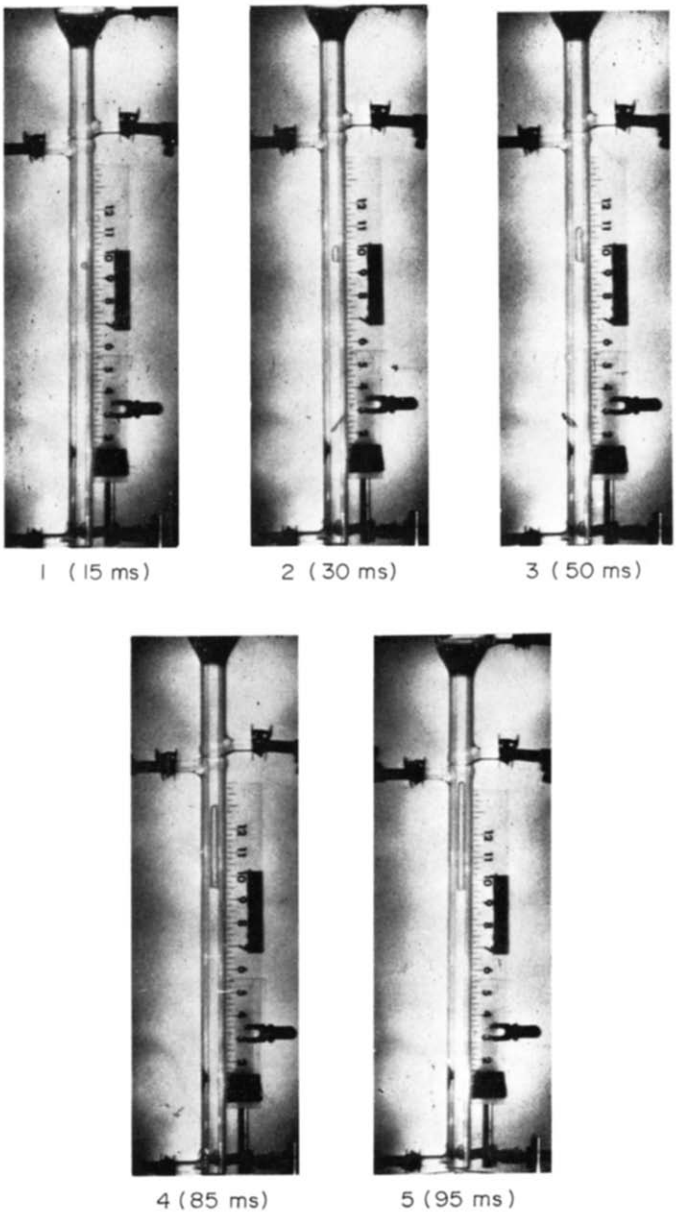


FIG. 4. Single channel expulsion illustrating various stages in void growth.

sure within the vapor space, under the assumption of equilibrium between the vapor and the liquid surface at every instant. This temperature, which must be guessed at each time interval, couples the energy and momentum equations.

A similar analysis may be performed on the film–vapor interface. The heat equation and corresponding boundary conditions become

$$\frac{\alpha\hat{c}^2 T[\sigma t, t_0(x)]}{\partial\sigma^2} = \frac{\partial T[\sigma, t, t_0(x)]}{\partial t} \tag{8}$$

subject to

$$T = T_w \text{ at } t = t_0 \text{ for all } \sigma, x \tag{9}$$

$$T = T_w \text{ at } \sigma = \infty \text{ for all } t, x \tag{10}$$

$$T = \phi(t) \text{ at } \sigma = 0 \text{ for all } t > t_0 \text{ and } x \tag{11}$$

where $t_0(x)$ is the time at which a fluid element at position $x$ was exposed to vapor. Equations (8)–(11) may be solved to yield

$$\left.\frac{dT[\sigma, t, t_0(x)]}{d\sigma}\right|_{\sigma=0} = \frac{\{T_w - \phi[t_0(x)]\}}{\sqrt{\{\pi\alpha[t - t_0(x)]\}}} - \int_{t_0}^{t} \frac{1}{\sqrt{[\pi\alpha(t - t_0 - \tau)]}} \frac{d\phi(\tau)}{d\tau} d\tau. \tag{12}$$

It is clear from equations (8)–(10) that it has been assumed that the thermal boundary layer is small with respect to the film thickness, and also that there is negligible drainage within the film.

The numerical solution proceeds by assuming the temperature at the liquid–vapor interface, which determines the pressure within the vapor region as the saturation pressure. Equations (2) and (3) are then integrated over one time-step to determine the new position of the upper interface.

Having determined the new interface position from the momentum equation, equation (4) can also be integrated to determine the new interface position from energy considerations. In evaluating the temperature gradient at the film–vapor interface, the time at which each increment was exposed is recorded. Equation (12) is then applied to each increment of film, and the energy released by that increment calculated. The contribution of each increment is summed over the length of the vapor space to determine the total energy contribution of the film.

If the position of the upper interface calculated from the momentum and energy equations were within a specified limit, the interface is assigned this new position; if not, a new interface temperature is assumed, and the calculations repeated.

## EXPERIMENTAL RESULTS

The expulsion experiment was performed for various superheats ranging from 59 to 128°F, and the results were compared with the numerical predictions.

Figures 6–9 show a comparison between the experimental data and the solution to equations (2)–(4). The limiting case of an energy controlled solution, in which the driving force is the temperature within the heated zone minus the saturation temperature corresponding to the plenum pressure, is also depicted. This solution accounts for the variation in the thermal boundary-layer thickness as a function of exposure time. It may be noted that the interface

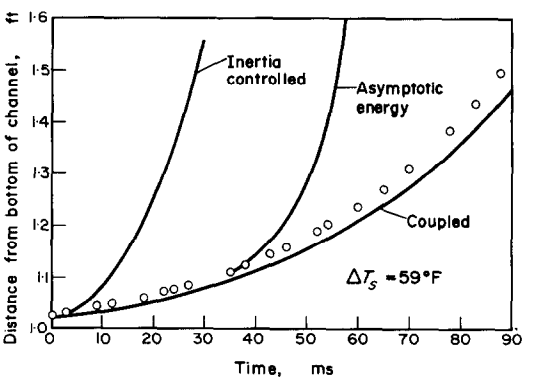


FIG. 6. Distance of upper liquid–vapor interface from bottom of channel vs. time for a slug expulsion at constant plenum pressure.

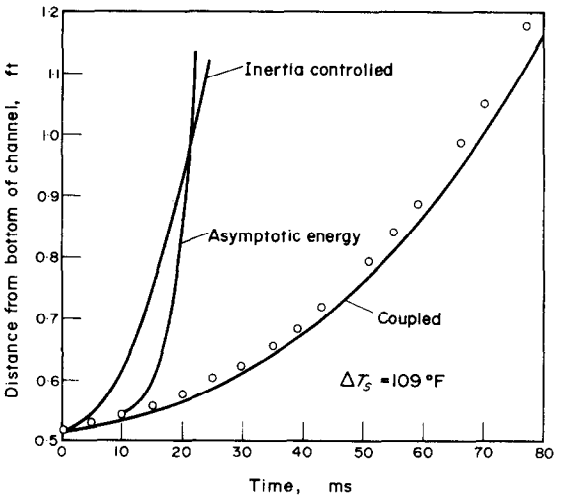


FIG. 7. Distance of upper liquid–vapor interface from bottom of channel vs. time for a slug expulsion at constant plenum pressure.

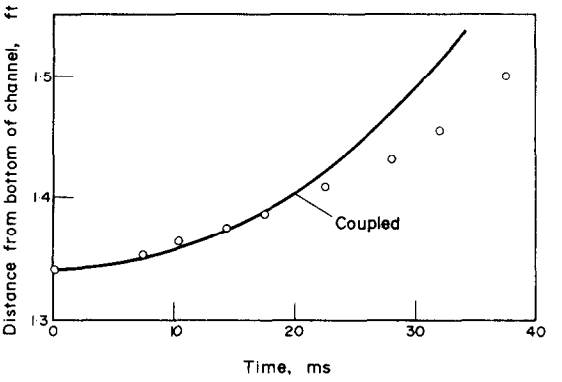


FIG. 9. Distance of upper liquid–vapor interface from bottom of channel vs. time for a slug expulsion with a varying plenum pressure.

velocity increases with time, both experimentally and theoretically, in contrast to spherical bubbles whose growth rates in uniformly superheated liquid decrease continuously with time. The difference in behavior may be ascribed to the continuous exposure of fresh interface in the slug geometry, as compared to the steady and uniform increase in thermal boundary-layer thickness in the spherical geometry. At the opposite limit, the inertia-controlled solution based upon a constant pressure driving force in the momentum equation is shown.

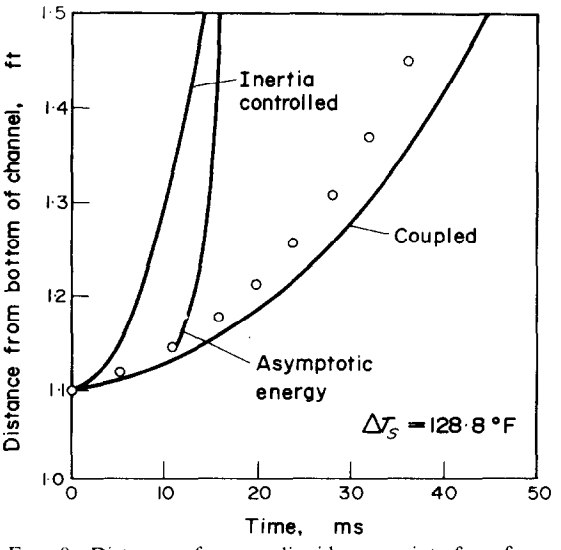


FIG. 8. Distance of upper liquid–vapor interface from bottom of channel vs. time for a slug expulsion at constant plenum pressure.

The thermal boundary-layer thickness calculated for the event shown in Fig. 8 was 0·012 mm, which is small in comparison with the film thickness found by Spiller *et al.* of 0·1 mm. Thus, the assumption of a thin thermal boundary layer seems to be satisfied.

In addition, it was assumed that drainage within the film was negligible. A calculation of the steady-state drainage velocity for the film in Fig. 7 shows an average velocity of 0·124 ft/s, which is small in comparison with the slug velocity of 10 ft/s. Hence, this assumption also appears to be valid.

Figure 9 depicts an event in which the void begins growing with a time-varying-plenum pressure. By comparing the pressure trace with the high-speed film, the pressure history during the growth of the void was determined. This pressure profile was inserted into the computer code, and the corresponding expulsion computed. The excellent agreement seems to support the physical model proposed herein.

## ACKNOWLEDGEMENTS

The authors are grateful to the Argonne Universities Association--Argonne National Laboratory for support during the course of this work. In addition, the helpful discussions with Dr. M. A. Grolmes and Mr. G. A. Lambert pertaining to the experimental portion of this work, and the assistance of Messrs. L. Bova and E. Gunchin in the construction and operation of the experimental facility, was appreciated.

## REFERENCES

1. K. H. SPILLER *et al.*, Superheating and single bubble ejection in the vaporization of stagnating liquid metals, *Atomkernenergie* **12** (3/4), 111–114 (1967).
2. A. W. CRONENBERG *et al.*, Simplified model for sodium coolant expulsion and re-entry, *Trans Am. Nucl. Soc.* **12**, 364 (1969).
3. E. G. SCHLECHTENDAHL, Die Ejektion von Natrium aus Reaktorkuhlkanalen, *Nukleonik* **10** (Nov. 1967).
4. P. G. KOSKY, Bubble growth measurements in uniformly superheated liquids, *Chem. Engng Sci.* **23**, 695–706 (1968).
5. M. S. PLESSET and S. A. ZWICK, The growth of vapor bubbles in superheated liquids, *J. Appl. Phys.* **25**, 493 (1954).
6. S. J. BOARD, Experimental observations of vapor bubble growth in various constrained geometries, Central Electricity Generating Board, RD/B/N1418, (July, 1969).
7. R. B. BIRD, W. E. STEWART and E. N. LIGHTFOOT, *Transport Phenomena.* John Wiley, New York (1960).
8. J. C. SLATTERY, unpublished notes.
9. R. C. DOWNING, Transport properties of freon fluorocarbons, Freon Technical Bulletin, No. C-30, E. I. Dupont de Nemours and Co. (Inc.).

## EXPULSION EN BLOC DU FRÉON 113 PAR DÉPRESSURATION RAPIDE DANS UN TUBE VERTICAL

**Résumé**—Des résultats expérimentaux correspondent à une surchauffe initiale comprise entre 32.8 et 71,2°C, sont obtenus pour l'expulsion en bloc de Fréon 113 depuis un canal de diam tre constant. En plus, on donne une analyse dans laquelle les équations d'énergie et de quantité de mouvement sont couplées numériquement. L'équation d'énergie tient compte non seulement de l'énergie transportée à travers les interfaces liquide-vapeur supérieure et inférieure, mais aussi de celle transportée à travers l'interface film-vapeur de la paroi. En calculant la contribution énergétique du film pariétal, une fine couche limite thermique superficielle est supposée exister, couche dont l'épaisseur est fonction du temps d'exposition et de la position le long de la région de vapeur. Les résultats expérimentaux et la solution sont en bon accord.

## DIE KOLBENAUSSTRÖMUNG VON FREON-113 BEI RASCHER DRUCKMINDERUNG IN EINEM SENKRECHTEN ROHR

**Zusammenfassung**—Es liegen experimentelle Ergebnisse für die Kolbenausströmung von Freon-113 aus einem Rohr von konstantem Durchmesser vor, wobei die anfängliche Überhitzung von 33 bis 71°C reicht. Zusätzlich wurden in einer Analyse die Energie- und Impulsbeziehungen numerisch gekoppelt. Die Energiegleichung gilt nicht nur für die Energie, die über die obere und untere Dampf-Flüssigkeits-Grenzschicht, sondern auch für jene, die über die Wand-Dampf-Schicht transportiert wird. Bei der Berechnung des Energieanteils des Wand-Films wurde eine dünne thermische Grenzschicht angenommen, deren Dicke als eine Funktion der Ausbildungszeit und der Stelle im Dampfraum angenommen wurde. Es zeigte sich gute Übereinstimmung zwischen den experimentellen Ergebnissen und der gekoppelten Lösung.

## СТЕРЖНЕВОЕ ВЫБРАСЫВАНИЕ ФРЕОНА-113 ПУТЕМ БЫСТРОГО ПОНИЖЕНИЯ ДАВЛЕНИЯ В ВЕРТИКАЛЬНОЙ ТРУБЕ

**Аннотация**—Получены экспериментальные данные для стержневого выбрасывания фреона-113 из канала с постоянным диаметром с начальным перегревом 59–128°*F*. Далее приводится численный анализ для уравнений энергии и количества движения. Уравнение энергии учитывает не только перенос энергии через верхнюю и нижнюю поверхности раздела жидкость-пар, но также и через границу раздела пар-пленка у стенки. При расчете энергии, проходящей через пленку у стенки, предполагается существование тонкого теплового пограничного слоя, толщина которого учитывается как функция времени прохождения и положения при прохождении вдоль пара. Найдено хорошее соответствие между экспериментальными данными и соответствующим решением.